Paper 94

Proceedings of the Eleventh International Conference
on Computational Structures Technology,
B.H.V. Topping, (Editor),
Civil-Comp Press, Stirlingshire, Scotland

An Equivalent Isotropic Model for Functionally Graded Plates

D. Kennedy and R.K.H. Cheng
Cardiff School of Engineering
Cardiff University, Wales, United Kingdom

Abstract

A functionally graded plate whose material properties vary continuously through the thickness is modelled as an equivalent isotropic plate with an offset neutral surface. The model gives an exact analogy if the matrix and reinforcement materials have the same Poisson's ratio, and otherwise a small approximation is introduced. The correctness and accuracy of the model are confirmed by comparing critical buckling and undamped free vibration results with well converged solutions from an approximate model in which the plate is divided into isotropic layers. Agreement is also demonstrated with theoretical predictions and results from the literature.

Keywords: functionally graded, plates, vibration, dynamic stiffness, isotropic, Wittrick-Williams algorithm.

1 Introduction

This paper considers the critical buckling and free vibration of functionally graded (FG) plates whose material properties vary continuously through the thickness. Such plates can be regarded as consisting of two phases, known as the matrix and reinforcement. The volume fraction of the reinforcement varies from zero to unity through the thickness of the plate, e.g. according to a power law, so that the composition is pure matrix material on the top surface and pure reinforcement material on the bottom surface. Applications include metal/ceramic components in aerospace and industrial applications which are required to withstand high temperature gradients [1].

Critical buckling loads and natural frequencies of FG plates have been tabulated by various authors [2-5], and it was shown by Abrate [6, 7] that these results are always proportional to those for homogeneous isotropic plates. Coupling between in-plane and out-of-plane behaviour can be eliminated by an appropriate choice of

the neutral surface [8-10]. Thus the behaviour of FG plates can be predicted from that of similar homogeneous plates.

In this paper, these ideas are extended to obtain an equivalent isotropic model for a FG plate so that it can be analysed using existing methods based on classical plate theory (CPT) for homogeneous plates. For the equivalent plate it is necessary to define the thickness, Young's modulus, Poisson's ratio and (for a vibration problem) the density. The position of the neutral surface is defined in terms of an offset above the geometric mid-surface. Expressions for these quantities are derived in Section 2, and are shown to give an exact equivalence when the matrix and reinforcement materials have the same Poisson's ratio; otherwise a small approximation is introduced. The numerical results in Section 3 serve to validate the proposed model, and also demonstrate its accuracy for both buckling and vibration problems. Section 4 summarises the conclusions and suggests some extensions to the method.

2 Analysis

2.1 Stiffness properties of a functionally graded plate

Consider a FG plate of thickness h lying in the xy plane with the origin at mid-surface, having material properties which vary through the thickness (z) direction. Using standard notation, the plate constitutive relations are written as

$$\mathbf{N} = \mathbf{A}\boldsymbol{\varepsilon}_0 + \mathbf{B}\boldsymbol{\kappa} \qquad\qquad \mathbf{M} = \mathbf{B}\boldsymbol{\varepsilon}_0 + \mathbf{D}\boldsymbol{\kappa} \tag{1}$$

where the vectors $\mathbf{N}$, $\mathbf{M}$, $\boldsymbol{\varepsilon}_0$ and $\boldsymbol{\kappa}$ contain perturbation membrane forces per unit length, perturbation bending and twisting moments per unit length, perturbation mid-surface membrane strains, and perturbation curvatures and twist, respectively; the membrane, coupling and out-of-plane stiffness matrices are given by

$$\mathbf{A} = \int_{-h/2}^{h/2} E(z)\mathbf{Q}(z)dz \quad \mathbf{B} = \int_{-h/2}^{h/2} E(z)\mathbf{Q}(z)zdz \quad \mathbf{D} = \int_{-h/2}^{h/2} E(z)\mathbf{Q}(z)z^2dz \tag{2}$$

respectively; and

$$\mathbf{Q}(z) = \begin{bmatrix} \dfrac{1}{1-\nu(z)^2} & \dfrac{\nu(z)}{1-\nu(z)^2} & 0 \\ \dfrac{\nu(z)}{1-\nu(z)^2} & \dfrac{1}{1-\nu(z)^2} & 0 \\ 0 & 0 & \dfrac{1}{2\big(1+\nu(z)\big)} \end{bmatrix} \tag{3}$$

Young's modulus $E(z)$, Poisson's ratio $\nu(z)$ and the material density $\rho(z)$ are each assumed to vary through the thickness according to the rule of mixtures

$$\begin{bmatrix} E(z) \\ \nu(z) \\ \rho(z) \end{bmatrix} = \begin{bmatrix} E_m \\ \nu_m \\ \rho_m \end{bmatrix} + V(z) \left\{ \begin{bmatrix} E_r \\ \nu_r \\ \rho_r \end{bmatrix} - \begin{bmatrix} E_m \\ \nu_m \\ \rho_m \end{bmatrix} \right\} \tag{4}$$

where subscripts m and r denote the properties of the metal and reinforcement, respectively; and $V(z)$ is the volume fraction of the reinforcement, which is commonly assumed to follow the power law

$$V(z) = \left(\frac{1}{2} + \frac{z}{h}\right)^n \tag{5}$$

The non-negative volume fraction index n controls the variation of the properties of the FG plate, as illustrated in Figure 1. As n approaches zero the plate consists essentially of reinforcement material, while as n approaches infinity it consists essentially of matrix material.

If both materials have the same Poisson's ratio $\nu_m = \nu_r = \nu_0$, then Equations (3) and (4) show that $\nu(z) \equiv \nu_0$ and

$$\mathbf{Q}(z) \equiv \mathbf{Q}_0 = \begin{bmatrix} \frac{1}{1-\nu_0{}^2} & \frac{\nu_0}{1-\nu_0{}^2} & 0 \\ \frac{\nu_0}{1-\nu_0{}^2} & \frac{1}{1-\nu_0{}^2} & 0 \\ 0 & 0 & \frac{1}{2(1+\nu_0)} \end{bmatrix} \tag{6}$$

Thus Equation (2) can be written as

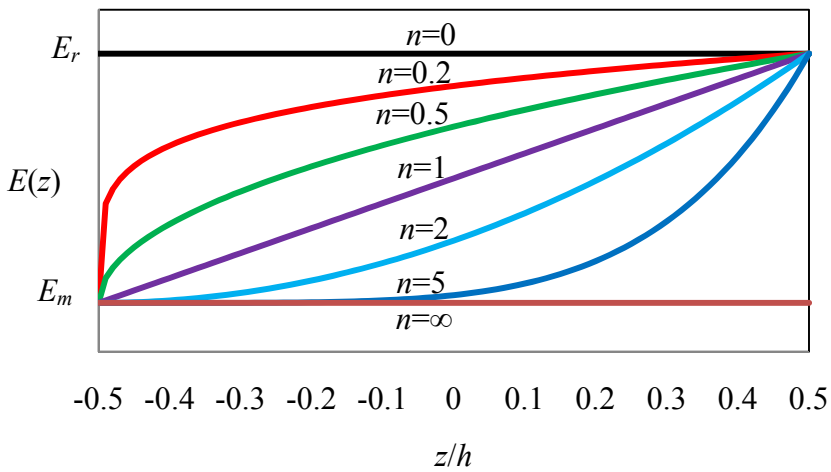

Figure 1. Variation of Young's modulus through the thickness of a FG plate with volume fraction index n

$$\mathbf{A} = \left[\int_{-h/2}^{h/2} E(z)dz\right]\mathbf{Q}_0 \quad \mathbf{B} = \left[\int_{-h/2}^{h/2} E(z)zdz\right]\mathbf{Q}_0 \quad \mathbf{D} = \left[\int_{-h/2}^{h/2} E(z)z^2dz\right]\mathbf{Q}_0 \tag{7}$$

and, on substitution for $E(z)$ from Equations (4) and (5),

$$\mathbf{A} = A_F\mathbf{Q}_0 \qquad \mathbf{B} = B_F\mathbf{Q}_0 \qquad \mathbf{D} = D_F\mathbf{Q}_0 \tag{8}$$

where

$$A_F = h\left(E_m + \frac{E_r - E_m}{n+1}\right) \qquad B_F = \frac{h^2}{2}\frac{n}{(n+1)(n+2)}(E_r - E_m)$$
$$D_F = \frac{h^3}{12}\left[E_m + \frac{3(n^2+n+2)}{(n+1)(n+2)(n+3)}(E_r - E_m)\right] \tag{9}$$

The presence of B_F indicates the introduction of coupling between the in-plane and out-of-plane behaviour.

2.2 Equivalent isotropic plate

Consider an isotropic plate of thickness h^*, Young's modulus E^*, Poisson's ratio $\nu^* = \nu_0$, whose neutral surface is offset by δ^* above the geometric mid-surface. This plate has membrane, coupling and out-of-plane stiffness matrices given by

$$\mathbf{A} = E^*h^*\mathbf{Q}_0 \qquad \mathbf{B} = E^*h^*\delta^*\mathbf{Q}_0 \qquad \mathbf{D} = E^*\left(\frac{h^{*3}}{12} + h^*\delta^{*2}\right)\mathbf{Q}_0 \tag{10}$$

and is therefore equivalent to the FG plate of Equation (8) if

$$\delta^* = \frac{B_F}{A_F} \qquad h^* = \sqrt{12\left(\frac{D_F}{A_F} - \frac{{B_F}^2}{{A_F}^2}\right)} \qquad E^* = \frac{A_F}{h^*} \tag{11}$$

For vibration analysis it is also necessary to define an equivalent density ρ^*, such that the mass per unit area ρ^*h^* of the equivalent plate is equal to that of the FG plate, i.e.

$$\rho^* = \left(\rho_m + \frac{\rho_r - \rho_m}{n+1}\right)\left(\frac{h}{h^*}\right) \tag{12}$$

Equations (11) and (12) give an exact isotropic equivalence for FG graded plates with constant Poisson's ratio. For cases where Poisson's ratio varies through the thickness of the plate, analytical solutions are not readily available for the integrations of Equation (2). For such cases an approximate solution is proposed in

which the Poisson's ratio for the equivalent isotropic plate is equated to the mean value for the FG plate, i.e.

$$\nu^* = \left(\nu_m + \frac{\nu_r - \nu_m}{n+1}\right) \tag{13}$$

2.3 Buckling and vibration analysis

Given any FG plate, Equations (11)-(13) define the dimensions and material properties of an isotropic plate, from which the **A**, **B** and **D** matrices can be constructed using Equation (10). Critical buckling loads and undamped natural frequencies, based on CPT, can then be found using any existing form of analysis for isotropic plates which allows for an offset between the neutral surface and the geometric mid-surface.

Alternatively, approximate solutions can be obtained by dividing the FG plate into a large number n_l of isotropic layers, each of thickness h/n_l, with the material properties for the ith layer given by Equation (4) with

$$z = \frac{h}{2}\left(-1 + \frac{2i-1}{n_l}\right) \tag{14}$$

and performing buckling or vibration analysis for the resulting laminated plate.

Both these forms of analysis are available in the exact strip software VICONOPT [11], which covers critical buckling, postbuckling and free vibration analysis, and optimum design, of prismatic plate assemblies. In the simplest form of the analysis [12], the mode of buckling or vibration is assumed to vary sinusoidally in the prismatic (or longitudinal) direction, giving exact solutions for isotropic and orthotropic stiffened plates and panels in the absence of shear load. Analytical or numerical solution of the governing differential equations in the transverse direction avoids the usual discretisation required by the finite element and finite strip methods. This approach yields a transcendental dynamic stiffness matrix which cannot be handled by conventional linear eigensolvers, but application of the Wittrick-Williams algorithm [13] permits reliable, accurate and rapid convergence on any required eigenvalue, i.e. critical buckling load or undamped natural frequency.

3 Numerical examples

3.1 Properties of equivalent isotropic plate

The first example considered here is a FG plate of thickness $h = 2\text{mm}$, composed of an aluminium matrix reinforced by ceramic material. The aluminium and ceramic have Young's modulus $E_m = 70\text{GPa}$ and $E_r = 121\text{GPa}$, respectively, and both materials have the same Poisson's ratio $\nu_m = \nu_r = \nu_0 = 0.25$. Figure 2 shows plots

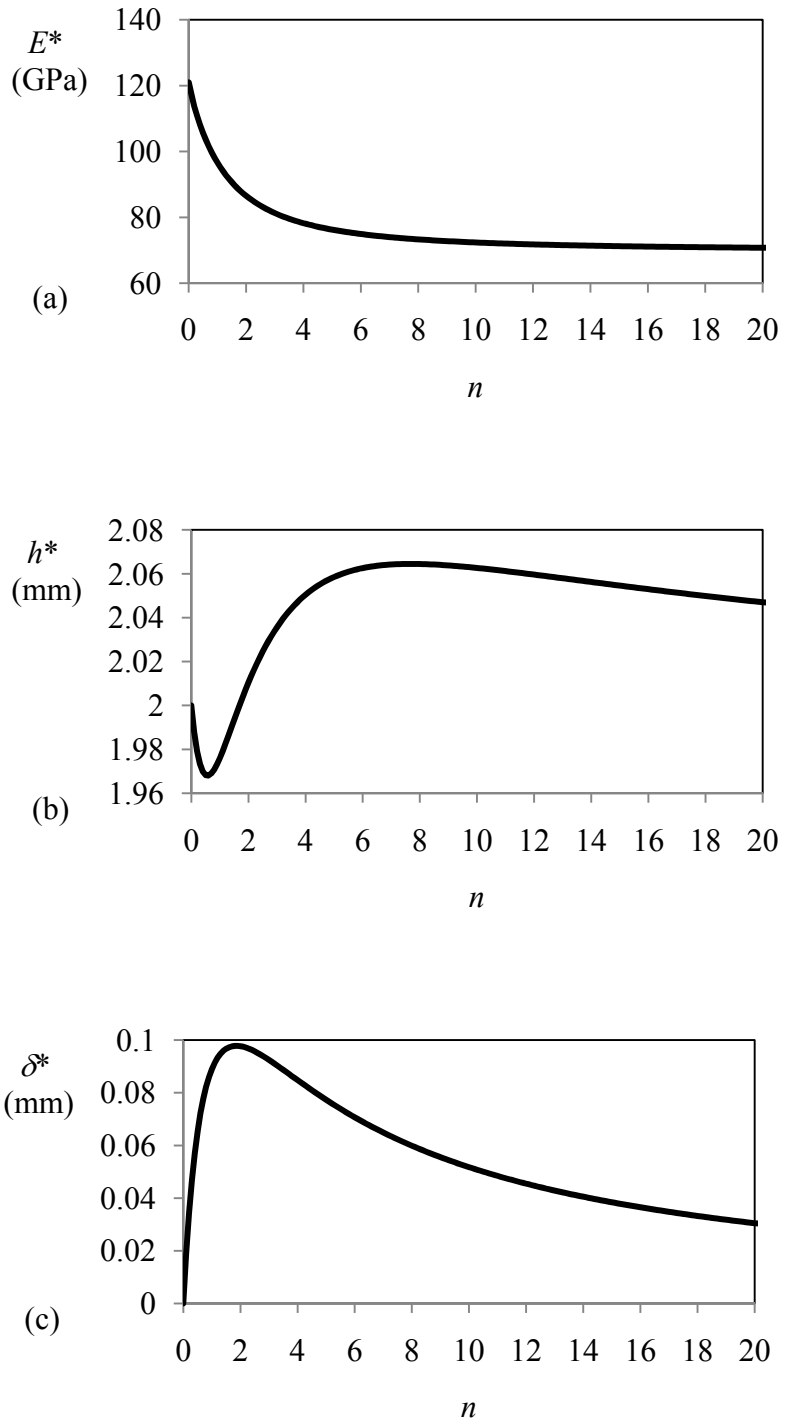

Figure 2. Plots of (a) equivalent Young's modulus E^*, (b) equivalent thickness h^*, and (c) neutral surface offset δ^* against volume fraction index n, for an aluminium-ceramic FG plate of thickness $h = 2\text{mm}$

of the Young's modulus E^*, thickness h^* and neutral surface offset δ^* of the equivalent isotropic plate, obtained using Equations (9) and (11) for different values of the volume fraction index n. Figure 2(a) demonstrates how the equivalent Young's modulus varies from that of the reinforcement material when $n = 0$ to that of the matrix material as n approaches infinity, in agreement with Figure 1 which shows that these represent extreme cases where the FG plate is composed of a single isotopic material.

For these two extreme cases, the equivalent isotropic plate is identical to the FG plate. Therefore it has thickness $h^* = h$ and its neutral surface coincides with the geometric mid-surface, i.e. $\delta^* = 0$, as shown in Figures 2(b) and 2(c), respectively. It is seen from Figure 2(b) that the thickness of the equivalent plate can be either larger or smaller than that of the FG plate, by up to about 3% for this example, depending on the value of n. Also, from Figure 2(c), the neutral surface of the equivalent plate is always offset above its geometric mid-surface, by up to 5% of the true thickness h. It can be shown analytically from Equations (9) and (11) that the greatest offset is given by

$$\delta^* = \frac{h}{2}\left[\frac{(E_r - E_m)}{\left(\sqrt{E_r} + \sqrt{2E_m}\right)^2}\right] \tag{15}$$

and occurs when $n = \sqrt{2E_r/E_m}$.

3.2 Critical buckling of a functionally graded plate

A simply supported square aluminium-ceramic FG plate of length $a = 100\text{mm}$, thickness $h = 2\text{mm}$ and the material properties given in Section 3.1 was loaded in uniform longitudinal compression. For seven values of the volume fraction index, ranging from $n = 0$ (i.e. pure ceramic) to $n = \infty$ (i.e. pure metal), the software VICONOPT was used to find the critical buckling load, firstly by using an analytical model of the equivalent isotropic plate defined in Section 2.2, and secondly by using an approximate layered model with up to $n_l = 128$ isotropic layers. The analytical results can be regarded as exact for this example because both materials have the same Poisson's ratio.

Figure 3 shows that the results from the layered model converge towards the analytical results as n_l is increased, giving 4 to 6 significant figures of accuracy when $n_l = 128$. Under the assumption of uniform convergence, a set of results $\{f_{n_l}\}$ from the layered model can be used to give an extrapolated prediction

$$\bar{f} = \frac{f_{32}f_{128} - (f_{64})^2}{f_{32} - 2f_{64} + f_{128}} \tag{16}$$

where f_{n_l} represents the result found for the approximate model with n_l layers. Table 1 shows that these predictions are even closer to the analytical results, demonstrating the correctness of the equivalent isotropic model.

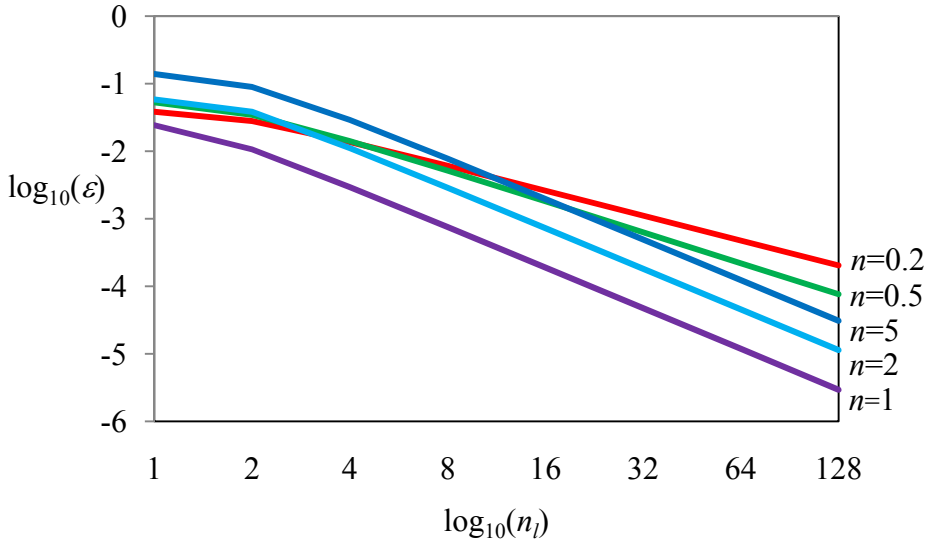

Figure 3. Relative errors in the critical buckling load of a square simply supported aluminium-ceramic FG plate with volume fraction index n, comparing a layered solution with n_l layers and the analytical solution for an equivalent isotropic plate

	P_{cr} (kN)			Relative error	
n	Analytical	Approximate	Extrapolated	Approximate	Extrapolated
0	33.96899	33.96899	33.96899	0.00	0.00
0.2	30.92865	30.93497	30.92874	2.04×10^{-4}	2.73×10^{-6}
0.5	28.27660	28.27876	28.27660	7.64×10^{-5}	3.18×10^{-7}
1	26.17307	26.17314	26.17306	2.94×10^{-6}	-5.53×10^{-8}
2	24.67906	24.67878	24.67906	-1.14×10^{-5}	-9.00×10^{-9}
5	23.34671	23.34599	23.34671	-3.10×10^{-5}	-4.71×10^{-9}
∞	19.65148	19.65148	19.65148	0.00	0.00

Table 1. Critical buckling load of a square simply supported aluminium-ceramic FG plate with volume fraction index n, comparing the analytical solution for an equivalent isotropic plate, the approximate layered solution with $n_l = 128$ layers, and extrapolations from the layered solutions obtained using Equation (16)

3.3 Natural frequencies of a functionally graded plate

Abrate [6] studied the free vibration of FG plates composed of a titanium alloy (Ti) matrix reinforced by aluminium oxide (AlOx). The titanium had Young's modulus $E_m = 349.55\text{GPa}$, Poisson's ratio $\nu_m = 0.26$ and density $\rho_m = 3750\text{kgm}^{-3}$, while the aluminium oxide had Young's modulus $E_r = 122.56\text{GPa}$, Poisson's ratio $\nu_r = 0.2884$ and density $\rho_r = 4429\text{kgm}^{-3}$.

The software VICONOPT was used to find the fundamental natural frequencies of simply supported square FG plates of this composition, with length $a = 100\text{mm}$ and thickness $h = 2\text{mm}$, for seven values of the volume fraction index, ranging from $n = 0$ (i.e. pure reinforcement) to $n = \infty$ (i.e. pure matrix). As in Section 3.2, results from an analytical model of the equivalent isotropic plate were compared with those from an approximate layered model with up to $n_l = 128$ isotropic layers, and with extrapolated predictions from the latter. Figure 4 shows agreement to approximately 4 significant figures between the analytical and approximate results.

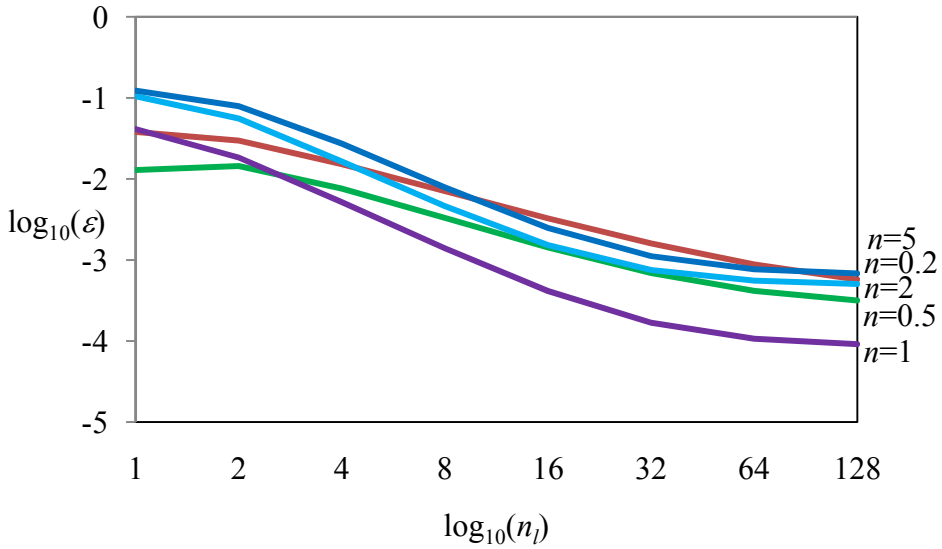

Figure 4. Relative errors in the fundamental natural frequency of a square simply supported AlOx-Ti FG plate with volume fraction index n, comparing a layered solution with n_l layers and the analytical solution for an equivalent isotropic plate

	ω_{11}			Relative error	
n	Analytical	Approximate	Extrapolated	Approximate	Extrapolated
0	996.477	996.477	996.477	0.00	0.00
0.2	1163.675	1163.006	1163.274	-5.75×10^{-4}	-3.45×10^{-4}
0.5	1279.568	1279.162	1279.234	-3.17×10^{-4}	-2.61×10^{-4}
1	1376.225	1376.351	1376.343	9.15×10^{-5}	8.63×10^{-5}
2	1472.185	1472.931	1472.907	5.07×10^{-4}	4.90×10^{-4}
5	1594.158	1595.245	1595.199	6.82×10^{-4}	6.53×10^{-4}
∞	1813.540	1813.540	1813.540	0.00	0.00

Table 2. Fundamental natural frequency of a square simply supported AlOx-Ti FG plate with volume fraction index n, comparing the analytical solution for an equivalent isotropic plate, the approximate layered solution with $n_l = 128$ layers, and extrapolations from the layered solutions obtained using Equation (16)

However, in contrast to the previous example, Table 2 shows that this accuracy cannot be significantly improved by extrapolation, indicating that as n_l is increased the layered model converges to natural frequencies which differ slightly from those of the equivalent isotropic plate. The reason for this is the approximation introduced by Equation (13) to obtain a constant value of Poisson's ratio for the equivalent isotropic model. Despite the loss of exactness, the discrepancy with well converged layered solutions is small enough to be neglected for practical purposes.

The natural frequencies ω_{ij} of a simply supported square isotropic plate of length a and thickness h, with Young's modulus E, Poisson's ratio ν and density ρ, are given by the expression [14]

$$\omega_{ij} = \frac{\pi h}{4a^2}\left[\sqrt{\frac{E}{3\rho(1-\nu^2)}}\right](i^2+j^2) \tag{17}$$

where i and j represent the number of half-waves in the longitudinal and transverse directions, respectively. Hence the natural frequencies can be written in the normalised form

$$\frac{\omega_{ij}}{\omega_{11}} = \frac{1}{2}(i^2+j^2) \tag{18}$$

Table 3 shows that this relationship is satisfied exactly for FG plates with extreme values of the volume fraction index $n = 0$ and $n = \infty$. The remaining cases in Table 3 were obtained using the equivalent isotropic model, and show slight discrepancies from the analytical results on account of the approximation in the representation of Poisson's ratio by Equation (13).

Finally, Table 4 lists the natural frequencies of Table 3, normalised with respect to ω_{11r}, the fundamental frequency of the FG plate with $n = 0$, i.e. composed of the AlOx reinforcement. This normalisation allows a comparison to be made with the results of [6], showing agreement to approximately 3 significant figures.

n	ω_{11}/ω_{11}	ω_{12}/ω_{11}	ω_{22}/ω_{11}	ω_{13}/ω_{11}	ω_{23}/ω_{11}	ω_{14}/ω_{11}
0	1.0000	2.5000	4.0000	5.0000	6.5000	8.5000
0.2	1.0000	2.4987	3.9960	4.9933	6.4881	8.4787
0.5	1.0000	2.4988	3.9962	4.9936	6.4886	8.4797
1	1.0000	2.4989	3.9964	4.9939	6.4892	8.4807
2	1.0000	2.4989	3.9965	4.9942	6.4896	8.4815
5	1.0000	2.4989	3.9965	4.9942	6.4896	8.4814
∞	1.0000	2.5000	4.0000	5.0000	6.5000	8.5000

Table 3. Natural frequencies ω_{ij} of a square simply supported AlOx-Ti FG plate with volume fraction index n, normalised with respect to the corresponding fundamental natural frequency ω_{11}

n		ω_{11}/ω_{11r}	ω_{12}/ω_{11r}	ω_{22}/ω_{11r}	ω_{13}/ω_{11r}	ω_{23}/ω_{11r}	ω_{14}/ω_{11r}
0	Present	1.0000	2.5000	4.0000	5.0000	6.5000	8.5000
	Ref. [6]	1.0000	2.4887	3.9106	4.9761	6.2964	8.4793
	Rel. diff.	0.00	4.53×10^{-3}	2.29×10^{-2}	4.81×10^{-3}	3.23×10^{-2}	2.44×10^{-3}
0.2	Present	1.1678	2.9180	4.6665	5.8311	7.5767	9.9014
	Ref. [6]	1.1713	2.9151	4.5805	5.8285	7.3749	9.9318
	Rel. diff.	-3.00×10^{-3}	1.00×10^{-3}	1.88×10^{-2}	4.53×10^{-4}	2.74×10^{-2}	-3.06×10^{-3}
0.5	Present	1.2841	3.2087	5.1314	6.4122	8.3319	10.8887
	Ref. [6]	1.2911	3.2132	5.0489	6.4246	8.1292	10.9477
	Rel. diff.	-5.42×10^{-3}	-1.40×10^{-3}	1.63×10^{-2}	-1.92×10^{-3}	2.49×10^{-2}	-5.39×10^{-3}
1	Present	1.3811	3.4512	5.5193	6.8971	8.9621	11.7126
	Ref. [6]	1.3875	3.4531	5.4259	6.9043	8.7362	11.7651
	Rel. diff.	-4.64×10^{-3}	-5.64×10^{-4}	1.72×10^{-2}	-1.05×10^{-3}	2.59×10^{-2}	-4.46×10^{-3}
2	Present	1.4774	3.6919	5.9044	7.3783	9.5877	12.5304
	Ref. [6]	-	-	-	-	-	-
	Rel. diff.	-	-	-	-	-	-
5	Present	1.5998	3.9977	6.3936	7.9896	10.3819	13.5685
	Ref. [6]	1.6032	3.9899	6.2695	7.9777	10.0944	13.5940
	Rel. diff.	-2.12×10^{-3}	1.95×10^{-3}	1.98×10^{-2}	1.50×10^{-3}	2.85×10^{-2}	-1.88×10^{-3}
∞	Present	1.8200	4.5499	7.2798	9.0998	11.8297	15.4696
	Ref. [6]	1.8185	4.5258	7.1114	9.0490	11.4499	15.4196
	Rel. diff.	7.93×10^{-4}	5.33×10^{-3}	2.37×10^{-2}	5.61×10^{-3}	3.32×10^{-2}	3.24×10^{-3}

Table 4. Natural frequencies ω_{ij} of a square simply supported AlOx-Ti FG plate with volume fraction index n, normalised with respect to the corresponding fundamental natural frequencies ω_{11r} of an AlOx plate

4 Conclusions and further work

An equivalent isotropic model has been developed for a functionally graded (FG) plate whose material properties vary continuously through the thickness. The model allows a FG plate to be analysed using existing methods based on classical plate theory for homogeneous plates with the neutral surface offset from the geometric mid-surface. Analytic expressions have been derived for the thickness, Young's modulus, Poisson's ratio and density of the equivalent isotropic plate. The model gives an exact analogy if the matrix and reinforcement materials have the same Poisson's ratio, and otherwise a small approximation is introduced.

The equivalent isotropic model has been validated by using the software VICONOPT to obtain critical buckling and undamped free vibration results for a simply supported square FG plate. The correctness and accuracy of the model have been confirmed by comparing these results with well converged solutions from an

approximate model in which the plate is divided into isotropic layers. Agreement has also been demonstrated with theoretical predictions and results from the literature.

Because the equivalent model can be used directly with established software such as VICONOPT, it will be a straightforward task to extend the present study to FG plates with different loading and support conditions, and to prismatic panels containing such plates, e.g. aircraft wing and fuselage panels. Attention will also be given to FG plates whose volume fraction varies in different ways through the thickness of the plate, and particularly to the accuracy of the results obtained when there is a significant difference between the Poisson's ratios of the matrix and the reinforcement materials.

The classical plate theory assumed in the present work gives satisfactory results for thin plates, but should be replaced by a more accurate (first or higher order) shear deformation theory when analysing thicker plates of the dimensions used in composite aircraft panels. It is proposed to extend the present study to obtain the additional material properties needed to analyse the equivalent isotropic model using the first order shear deformation theory currently available in VICONOPT.

References

[1] Y. Miyamoto, W.A. Kaysser, B.H. Rabin, A. Kawasaki, R.G. Ford, "Functionally Graded Materials: Design, Processing and Applications", Kluwer Academic Publishers, Dordrecht, Netherlands, 1999.

[2] K.M. Liew, J. Yang, S. Kitipornchai, "Postbuckling of piezoelectric FGM plates subject to thermo-electro-mechanical loading", International Journal of Solids and Structures, 40(15), 3869-3892, 2003.

[3] J. Yang, H.-S. Shen, "Dynamic response of initially stressed functionally graded rectangular thin plates", Composite Structures, 54(4), 497-508, 2001.

[4] X.Q. He, T.Y. Ng, S. Sivashanker, K.M. Liew, "Active control of FGM plates with integrated piezoelectric sensors and actuators", International Journal of Solids and Structures, 38(9), 1641-1655, 2001.

[5] J. Yang, H.-S. Shen, "Vibration characteristics and transient response of shear-deformable functionally graded plates in thermal environments", Journal of Sound and Vibration, 255(3), 579-602, 2002.

[6] S. Abrate, "Free vibration, buckling, and static deflections of functionally graded plates", Composites Science and Technology, 66(14), 2382-2394, 2006.

[7] S. Abrate, "Functionally graded plates behave like homogeneous plates", Composites: Part B, 39(1), 151-158, 2008.

[8] T. Morimoto, Y. Tanigawa, R. Kawamura, "Thermal buckling of functionally graded rectangular plates subjected to partial heating", International Journal of Mechanical Sciences, 48(9), 926-937, 2006.

[9] D.G. Zhang, Y.H. Zhou, "A theoretical analysis of FGM thin plates based on physical neutral surface", Computational Materials Science, 44(2), 716-720, 2008.

[10] T. Prakash, M.T. Singha, M. Ganapathi, “Influence of neutral surface position on the nonlinear stability behavior of functionally graded plates”, Computational Mechanics, 43(3), 341-350, 2009.
[11] D. Kennedy, C.A. Featherston, “Exact strip analysis and optimum design of aerospace structures”, The Aeronautical Journal, 114(1158), 505-512, 2010.
[12] W.H. Wittrick, F.W. Williams, “Buckling and vibration of anisotropic or isotropic plate assemblies under combined loadings”, International Journal of Mechanical Sciences, 16(4), 209-239, 1974.
[13] W.H. Wittrick, F.W. Williams, “A general algorithm for computing natural frequencies of elastic structures”, Quarterly Journal of Mechanics and Applied Mathematics, 24(3), 263-284, 1971.
[14] C.F. Beards, “Structural Vibration: Analysis and Damping”, Elsevier, Oxford, 1996.